[12] G. Salama, "Optical measurement of transmembrane potential in heart," in L. Loew (Ed.) *Spectroscopic Membrane Probes*, vol. 3. Boca Raton, FL, CRC Press, 1988.

[13] W. Muller, H. Windish, and H. A. Tritthart, "Fast optical monitoring of microscopic excitation patterns in cardiac muscle," *Biophys. J.*, vol. 56, pp. 623–629, 1989.

[14] R. Plonsey. The use of a bidomain model for the study of excitable media. *Lectures on Mathematics in The Life Sciences*, vol. 21, pp. 123–149, 1989.

[15] B. J. Roth, "Action potential propagation in a thick strand of cardiac muscle," *Circ. Res.*, vol. 68, pp. 162–173, 1991.

[16] C. S. Henriquez and R. Plonsey, "Simulation of propagation along a bundle of cardiac tissue. I. Mathematical formulation," *IEEE Trans. Biomed. Eng.*, vol. 37, pp. 851–860, 1990.

[17] B. J. Roth and J. P. Wikswo, Jr., "A bidomain model for the extracellular potential and magnetic field of cardiac tissue," *IEEE Trans. Biomed. Eng.*, vol. 33, pp. 467–469, 1986.

[18] C. S. Henriquez, N. Trayanova, and R. Plonsey, "Potential and current distributions in a cylindrical bundle of cardiac tissue," *Biophys. J.*, vol. 53, pp. 907–918, 1988.

[19] L. Clerc, "Directional differences of impulse spread in trabecular muscle from mammalian heart," *J. Physiol.*, vol. 255, pp. 335–346, 1976.

[20] J. D. Jackson, *Classical Electrodynamics*. New York: Wiley, 1975.

[21] K. W. Altman and R. Plonsey, "Development of a model for point source electrical fibre bundle stimulation," *Med. Biol. Eng. Comput.*, vol. 26, pp. 466–475, 1988.

Nonlinear Transforms of ECG Signals for Digital QRS Detection: A Quantitative Analysis

Seth Suppappola and Ying Sun

Abstract— A class of algorithms has been developed which detects QRS complexes in the electrocardiogram (ECG). The algorithms employ nonlinear transforms derived from multiplication of backward differences (MOBD). The algorithms are evaluated with the American Heart Association ECG database, and comparisons are made with the algorithms reported by Okada and by Hamilton and Tompkins. The MOBD algorithms provide a good performance tradeoff between accuracy and response time, making this type of algorithm desirable for real-time microprocessor-based implementation.

I. INTRODUCTION

Since the QRS complex marks the beginning of the left ventricular contraction, detection of this event has many clinical applications. With the rapid growth of computer technology, more and more medical instruments nowadays are microprocessor based. And in particular, digital QRS detection systems offer many advantages over analog platforms [1].

The purpose of this study is to characterize the role of nonlinear transforms in the QRS detection algorithms. The task is made difficult by the infinite number of possible forms for nonlinear operations and the lack of an effective mathematical tool for the analysis of nonlinear operations in the time domain.[1] We approach

[1] Classical Fourier analysis, for example, is limited to linear time-invariant systems and has very limited applications to this problem.

this problem by 1) evaluating the effects of a group of nonlinear transforms on QRS detection with the American Heart Association (AHA) ventricular arrhythmia ECG database and 2) comparing our detection algorithms to two other algorithms reported in the literature.

II. QRS DETECTION ALGORITHMS

There are three QRS detection algorithms under investigation: 1) The multiplication of backward difference (MOBD) algorithms [1], which we propose; 2) the Okada algorithm [2], selected due to its fast response; and 3) the Hamilton–Tompkins algorithm [3], chosen for its high accuracy.

The Okada algorithm and the Hamilton–Tompkins algorithm among other algorithms perform a squaring of the backward difference of the signal or compute an approximation to the actual derivative via a differentiating filter. The motivation for using such a procedure is derived from the inherent characteristic of the QRS complex to have high frequency content relative to the rest of the ECG. The difference or derivative of the QRS hence yields a larger value than that of the remainder of the signal. A squaring operation exploits this feature by amplifying the larger differences more than smaller differences, yet doing so in an exponential fashion.

The MOBD algorithms take the exploitative capabilities of squaring one step further [1]. Instead of squaring the difference, these algorithms multiply successive differences together. In doing so, more information indicating the occurrence of a QRS complex is utilized. This is the case since not only does the QRS complex have a high frequency content, but it is also characterized by large amplitude.

III. NONLINEAR TRANSFORMATION

All of the nonlinear transforms operate on some form of the derivative of the ECG. These nonlinear transforms are described as follows. We shall use $y[n]$ for the resulting nonlinear transformation at time n.

A. MOBD:

Let $x[n]$ denote the first-order backward difference at time n

$$x[n] = u[n] - u[n - 1] \qquad (1)$$

where $u[n]$ is the ECG data sample. We define the Nth-order MOBD nonlinear transform as

$$y[n] = \prod_{k=0}^{N-1} |x[n - k]|. \qquad (2)$$

Furthermore, if the sign consistency contraint is imposed, $y[n]$ is forced to be zero if the backward differences are not in agreement with respect to sign. That is,

$$y[n] = 0, \quad \text{if } \mathrm{sgn}(x[n - k]) \neq \mathrm{sgn}(x[n - (k + 1)]),$$
$$k = 0, 1, \cdots, N - 2 \qquad (3)$$

where $\mathrm{sgn}(x)$ is the signum function, returning ± 1 according to the sign of x and 0 at the discontinuity at the origin.

Henceforth, we use the shorthand notation MOBD(N), with N indicating the order of the nonlinear transform, followed by the words "sign consistent" if the sign consistency constraint is imposed.

B. Okada:

The Okada algorithm [2] uses as its "derivative" the difference between the low-pass filter preprocessing stage output $x_{\mathrm{LPF}}[n]$ and

a geometric mean of these outputs $\overline{x}_{\rm LPF}[n]$ centered about n. The nonlinear transform it uses is

$$y[n] = (x_{\rm LPF}[n] - \overline{x}_{\rm LPF}[n])^2. \tag{4}$$

C. Hamilton–Tompkins:

The Hamilton–Tompkins algorithm [3] computes an approximation to the derivative using an FIR filter, the output of which we denote $x_{\rm der}[n]$. The nonlinear transform it uses is

$$y[n] = x^2_{\rm der}[n]. \tag{5}$$

Note that in all the algorithms, the resulting transform is either positive or 0; therefore all waveforms undergo a type of full-wave rectification. The polarity of the ECG waveform hence becomes irrelevant. Thus the transformation can be viewed as a measure of QRS complex signal energy, thereby permitting easy comparison of this value (or a processed form of it) to a threshold to determine if the amount of "energy" is sufficient to have resulted from a QRS complex.

IV. DECISION PROCESS

All of the detectors in this study implement, as their final decision stage, a thresholding operation, essentially comparing the processed ECG signal to a threshold, which when surpassed results in an attempt for the detector to assert that a QRS complex has occurred. All the detectors implement a refractory period as well, which is a period of latency immediately following a QRS detection in which no additional detection may occur, even if the threshold is exceeded. This condition is justly applied due to a physiological constraint imposed by the refractory period of the cardiac muscle itself. Of the three types of algorithms, the Okada algorithm implements the least number of heuristic conditionals; however, it is not the least mathematically intensive. The Hamilton–Tompkins algorithm is, by far, the most complex of the three. It implements extensive filtering and an intricate decision process with many conditionals. Compared to the other algorithms, the MOBD algorithm processes the ECG with the least amount of computation.

Conceptually, the flow of the MOBD algorithm is as follows: 1) quantize the data to fewer bits. 2) Compute the processed signal based on the MOBD nonlinear transforms. 3) Decrement, by half, a time-decaying adaptive threshold, but not to the extent that it decays below the average noise level. This is done every 100 ms beginning with the culmination of the latest refractory period. 4) Compare the processed signal to the adaptive threshold. If exceeded, and not in the refractory period, then assert that a QRS complex has occurred and enter the refractory period (100 ms). 5) Outside the refractory period, the geometric mean of the processed signal is computed as a measure of the noise in the ECG for the current RR interval. This mean value is then added to half the average noise level to yield the new average noise level. 6) At the termination of the refractory period, reset the adaptive threshold to the maximum of the processed signal that occurred during the refractory period.

The order of the MOBD nonlinear transform is dependent on the sampling frequency. As of yet, we do not have a quantitative way to choose the optimal order, and must do so via experimentation. Thus we restrict the discussion in this paper to the performance at a 250-Hz sampling frequency as this is the sampling frequency of the AHA ECG database.

V. PERFORMANCE EVALUATION

To analyze and compare the various algorithms in an unbiased fashion, the entire content of the American Heart Association Ventric-
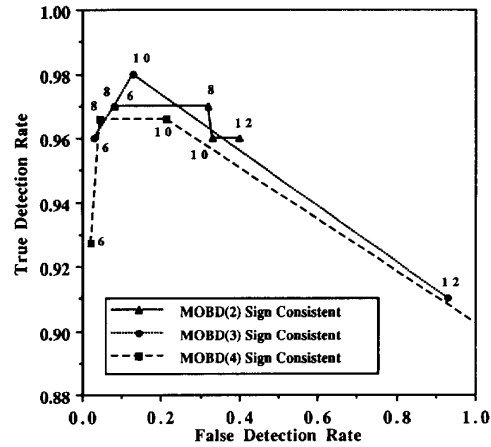

Fig. 1. Receiver operating characteristics for MOBD algorithms.

ular Arrhythmia Database (AHA ECG database) is used. The digital version of the AHA ECG database contains over 40 h of annotated dual-channel ECG recordings quantized to 12 bits at 250 Hz. In this study the two channels are treated as independent; all algorithms operate on a single stream of data. In other words, the correlation between the two channels is not exploited as an effort to increase the effectiveness of QRS detection. An analysis software developed on an IBM PC compatible computer is used to run each algorithm through the entire database. Both the algorithms and the analysis software are implemented in the C language.

The analysis software operates in an automated fashion. The performance statistics are accumulated based on a valid detection interval (VDI), which begins 50 ms before and ends 100 ms after the annotation time mark [1]. To avoid penalizing an algorithm with a slow response, the VDI is shifted by the processing delay for each algorithm. We have experimentally measured the average detection delay: 12 ms for the MOBD(4) sign consistent algorithm, 38 ms for the Okada algorithm, and 312 ms for the Hamilton–Tompkins algorithm.

If the algorithm fails to assert that a QRS complex has occurred at some point within the VDI, a false negative (FN) is declared. If the algorithm asserts that a QRS complex has occurred outside the VDI, a false positive (FP) is declared. Furthermore, a detector is allowed to assert the presence of a QRS complex only once during a VDI; otherwise, an FP will be declared for each extra detection. The receiver operating characteristics (ROC) curve [4] is established by plotting the true detection rate (TDR) versus the false detection rate (FDR), where TDR is given by 1 minus the FN rate and FDR is given by the FP rate. The quantization level is the variable along each ROC curve. The quantization level can be considered as a gain factor. The original quantization level of the AHA ECG database is 12 bits. By dropping bits of the sampled data from the least significant side (shifting right), the equivalent effect of decreasing input gain is created. The upper-left corner of the ROC plot (where TDR = 1 and FDR = 0) gives the optimal detection performance. An algorithm that has the ROC curve closer to the upper-left corner is considered a better algorithm than one that has the ROC curve farther away from the upper-left corner. Along the same ROC curve performance tradeoffs between FP's and FN's can be made. To obtain a single index related to the accuracy of QRS detection, we use a detection error rate defined by weighting FP's and FN's equally, i.e., the % detection error is given by the sum of the FP rate and the FN rate.
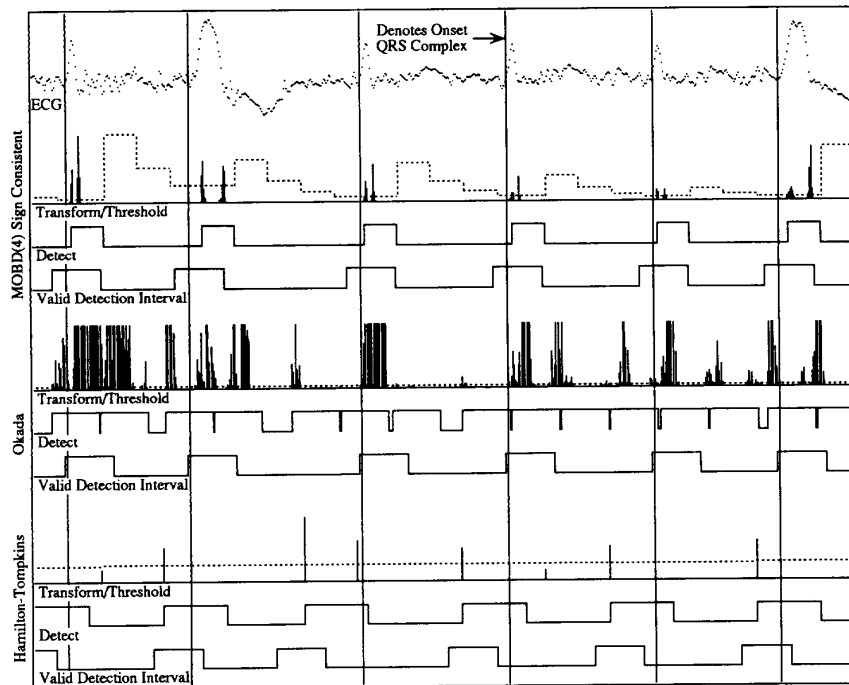
Fig. 2. Detection results (tape 4207, channel 1) from MOBD(4) sign consistent, Okada, and Hamilton–Tompkins algorithms.
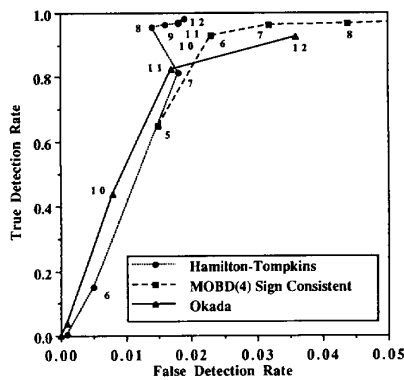

Fig. 3. Receiver operating characteristics for MOBD(4) sign consistent, Okada, and Hamilton–Tompkins algorithms.

TABLE I
MINIMUM ERROR RATE

Algorithm	Data Bits	FP	FN	% Error Rate†
MOBD(4) sign consistent	7	11633	13253	6.94
Okada	12	13066	26510	11.04
Hamilton–Tompkins	12	6746	7068	3.85

†Total beats analyzed: 358551.

The time required to pass the entire ECG database, one channel at a time, through each of the detection algorithms was 6.1 h for MOBD, 10.4 h for Okada, and 9.2 h for Hamilton–Tompkins. The analysis overhead including accessing the database and tallying the statistics was estimated to be 4.7 h. Thus the relative computational complexity was 1.0 for MOBD, 4.1 for Okada, and 3.2 for Hamilton–Tompkins. While only integer (16-bit) operations were used in the MOBD algorithm, long integer (32-bit) operations were necessary for both the Okada and the Hamilton–Tompkins algorithms.

VI. RESULTS

In Fig. 1 the ROC curves are established for three MOBD algorithms as the quantization level varies between 6 and 12 bits. It also shows that the MOBD(4) sign consistent algorithm gives the best performance around 8-bit quantization and is superior to the rest of the MOBD algorithms.

In Fig. 2, a particularly noisy segment of ECG is shown to compare the noise rejection capability among the three different algorithms. Notice that the Okada algorithm, showing many FP's, is relatively susceptible to noise. In Fig. 3 the ROC curves are shown for the three algorithms. It shows that the best quantization for the MOBD, Okada, and Hamilton–Tompkins algorithms are 7, 12, and 12 bits, respectively. At their best performance points, the accuracy ranking, from best to worst, is Hamilton–Tompkins, MOBD, and Okada (see Table I for performance statistics).

VII. DISCUSSION

From the preceding results, it is clear that of the three real-time QRS detection algorithms investigated in this study, no single algorithm proves to be preeminent. We find that there is a tradeoff between response time and accuracy. To make a decision about the presence of a QRS complex in real time, it is obviously less accurate to observe the ECG waveform only up to the peak of the QRS complex than to observe the entire appearance of the QRS complex. In other words, accuracy is gained by gathering more information at the sacrifice of response time. The Hamilton–Tompkins is most accurate with a 4% detection error; however, it suffers from a very slow response with the detection point at an average of 312 ms after the onset of the R-wave. The MOBD(4) sign consistent algorithm shows a 7% detection error and the fastest response with a 12-

ms response time. The Okada algorithm does not prevail in either category, with an 11% detection error and a 36-ms response time; it is, however, the easiest one to implement. As to the computational complexity, the Okada algorithm is 4.1 times higher than the MOBD algorithm; the Hamilton–Tompkins is 3.2 times higher than the MOBD algorithm.

A very interesting characteristic of the MOBD algorithm is that, to an extent, it uses the quantization effect for improving the signal to noise ratio and consequently, reduces the adverse effects of the noisy differencing operation. As shown in Fig. 3, the Okada algorithm primarily works with 12-bit quantization; its performance degrades drastically with fewer bits. The Hamilton–Tompkins algorithm was found to maintain good performance for quantization between 8 and 12 bits, with its best performance at 12 bits. In contrast, the best performance for the MOBD algorithm is with 7-bit quantization. As the number of bits increases, in all three cases, the number of FP's increases. This is not unusual because we could easily achieve 0 FP's by quantizing all the data to 0 bits (i.e., no signal). However, the analogy is not true for FN's. In the Okada and Hamilton–Tompkins algorithms, as the number of data bits increases, the number of FN's decreases. This is the intuitive result, as more data bits implies less quantization error and, thus, a more accurate representation of the ECG signal. In contrast, with the MOBD algorithm, as the number of bits increases, the number of FN's decreases to a point, but then increases drastically.

The MOBD algorithm's preference of fewer data bits can be exploited to increase the dynamic range of QRS detection. This can be accomplished by an implementation analogous to an automatic gain control: With "normal" input magnitude of the ECG signal, five right shifts are performed to reduce the sample word length from 12 to 7 bits. When the input magnitude decreases, the number of right shifts is decreased accordingly to maintain the desirable quantization level. An increase of the dynamic range by 30 dB is therefore achieved.

This study provides a quantitative analysis of using an unconventional nonlinear transform, multiplication of backward differences, in the context of QRS detection. The MOBD algorithm shows an extremely fast response and a reasonable accuracy; it should be suitable for those real-time applications in which detection of the presence of the QRS complex must be made while it is occurring.

REFERENCES

[1] Y. Sun, S. Suppappola, and T. A. Wrublewski, "Microcontroller-based real-time QRS detection," *Biomed. Instrum. Technol.,* vol. 26, no. 6, pp. 477–484, 1992.
[2] M. Okada, "A digital filter for the QRS complex detection," *IEEE Trans. Biomed. Eng.,* vol. BME-26, pp. 700–703, 1979.
[3] P. S. Hamilton and W. J. Tompkins, "Quantitative investigation of QRS detection rules using the MIT/BIH arrhythmia database," *IEEE Trans. Biomed. Eng.,* vol. BME-33, pp. 1157–1165, 1986.
[4] O. Pahlm and L. Sörnmo, "Software QRS detection in ambulatory monitoring—A review," *Med. Biol. Eng. Comput.,* vol. 22, pp. 289–297, 1984.

A CMOS Integrated Circuit for Multichannel Multiple-Subject Biotelemetry Using Bidirectional Optical Transmissions

Shoji Kawahito, Susumu Ueda, Makoto Ishida, Tetsuro Nakamura, Shiro Usui and Shunji Nagaoka

Abstract—A CMOS integrated circuit for a noninvasive biological-signal telemetry system specified for use in medical and physiological studies of the influence of weightlessness in space is presented. The system can monitor multichannel (4 channels maximum) biological signals from multiple subjects (4 subjects maximum) in real time by using time multiplexing. A key technique, so-called synchronized multiple-subject telemetry, to achieve multiple-subject telemetry has been proposed. This technique utilizes bidirectional optical transmissions with direct and scattered infrared lights between an observer and each of the subjects. An experimental CMOS IC to give a small light-weight low-power, and smart telemetry instrument for use on animals has been developed. This IC is for evaluating circuit blocks of the implantable monolithic telemetry instrument. The major circuit blocks include CMOS digital circuits for synchronization, subject selection and time multiplexing, analog circuits for pulse interval modulation (PIM), and other blocks such as a CMOS optical pulse receiver and an LED driver. A preliminary experimental multichannel telemetry from two subjects has been performed with the implemented IC chips, and the principal operation of the multiple-subject optical biotelemetry has been demonstrated.

I. INTRODUCTION

As space development advances, the continuous noninvasive monitoring of the physiological state of human or animal subjects becomes increasingly important not only for astronautics, but also with regard to studies of the effect of weightlessness. The development of a noninvasive physiological-state monitoring system, or biotelemetry system, is intensively required for supporting such a study [1], [2], [3]. The biotelemetry system used in space should meet the following requirements:

1) it should utilize small light-weight low-power equipment for use with small animals;
2) it should provide telemetry of multichannel biological signals from multiple subjects when we consider that there are differences between individual animals [2];
3) noninvasive monitoring must be possible; and
4) it is desired to be electromagnetic interference free.

In order to meet these requirements, the application of microelectronics is essential especially from the viewpoint of realizing small light-weight and low-power implantable telemeters. In fact, many IC-based implantable telemeters have been reported [4], [5]. The application of microelectronics is also attractive for realizing versatile telemeters. A multichannel telemeter is a typical example [6].

In this paper, we describe a CMOS integrated circuit specified for the aforementioned biotelemetry system. For the real-time monitoring multichannel biological signals from multiple animal subjects,